HO· and DNase I Probing of Eσ^{70} RNA Polymerase−λP$_R$ Promoter Open Complexes: Mg^{2+} Binding and Its Structural Consequences at the Transcription Start Site†

Maria L. Craig,‡ Won-Chul Suh,§,|| and M. Thomas Record, Jr.*,‡,§

Departments of Biochemistry and Chemistry, University of Wisconsin−Madison, Madison, Wisconsin 53706

Received August 21, 1995; Revised Manuscript Received October 20, 1995⊗

ABSTRACT: Chemical and enzymatic probing (footprinting) of the reactivity of the promoter DNA backbone is applied to characterize two binary open complexes, RP$_{o1}$ (−Mg^{2+}) and RP$_{o2}$ (+Mg^{2+}), formed by *Escherichia coli* RNA polymerase (Eσ^{70}) at the λP$_R$ promoter. We report that HO· detects major differences in backbone reactivity between RP$_{o1}$ and RP$_{o2}$ in the open region from −4 to +1 relative to the transcription start site. Deoxyribose sugars at positions −4 to +1 of the **t** (template) strand react with HO· in RP$_{o2}$ but are relatively protected in RP$_{o1}$. Binding of Mg^{2+} to convert RP$_{o1}$ to RP$_{o2}$ therefore increases the reactivity of two negatively charged footprinting agents [MnO$_4^-$; Suh, W.-C., Ross, W., & Record, M. T., Jr., (1993) *Science 259*, 358−361; and Fe(EDTA)$^{2-}$/HO·] at the start site and is required for binding of the negatively-charged initiating nucleotides to the polymerase and the **t** strand at the start site. We propose that these effects result from binding of two Mg^{2+} ions to the catalytic carboxyls in the nucleotide binding sites. Except for the key region on the **t** strand at the start site, the promoter DNA of both RP$_{o1}$ and RP$_{o2}$ is continuously protected from DNase I and hydroxyl radical (HO·) cleavage between the −12 and +25 promoter positions. Protection in the upstream region, extending from −13 to about −70, is periodic, with an 11 base pair periodicity indicative of binding of polymerase to a single face of the DNA helix. Since the backbone of approximately 6−7 of every 11 base pairs are protected, binding may involve a relatively deep surface groove of Eσ^{70}. Major enhancements of HO· and DNase I cleavage at −38 and −48 suggest bending-induced distortion of the double helix, consistent with a model in which the upstream region of the promoter DNA is wrapped around Eσ^{70}. Mg^{2+} binding in the RP$_{o1}$ → RP$_{o2}$ conversion causes changes in the extent of the HO· enhancements. Structural models for the two open complexes at λP$_R$ are discussed and compared in the context of RP$_{o2}$ (+Mg^{2+}) at different promoters.

Kinetic studies of the formation of the final binary open complex (RP$_{o2}$) between *Escherichia coli* RNA polymerase (Eσ^{70}) and the λP$_R$ promoter first suggested the existence of an intermediate open complex (RP$_{o1}$) and indicated that ~3 Mg^{2+} ions are required for the transition from RP$_{o1}$ to RP$_{o2}$ (Suh et al., 1992). Neither negative supercoiling nor increased temperature is sufficient to drive this conversion in the absence of Mg^{2+} at mM concentration (Suh et al., 1993). This specific requirement for Mg^{2+} uptake in the RP$_{o1}$ → RP$_{o2}$ conversion contrasts with the nonspecific competitive role of cations (including Mg^{2+}) in two preceding steps which affect the local phosphate charge density of promoter DNA.

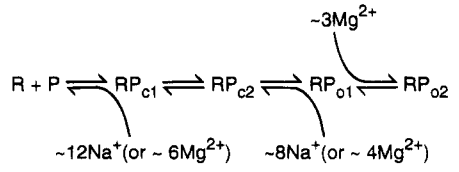

KMnO$_4$ probing in the presence and absence of Mg^{2+} showed that the two complexes differ in the extent of DNA base accessibility in the melted region surrounding the transcription start site (+1; Suh et al., 1993). A key difference between the two complexes is that the start site base on the **t** (template) strand is accessible to MnO$_4^-$ in RP$_{o2}$ but not in RP$_{o1}$. Do these differences result from Mg^{2+} binding at the start site? Does Mg^{2+} binding have effects distant from the start site? Does Mg^{2+} binding affect structure and/or local charge densities in the Eσ^{70}−promoter complex? What differences in accessibility of the DNA backbone exist between the two complexes? To address these questions, we have employed HO· and DNase I to footprint the **n** (nontemplate) and **t** strands of the DNA backbone in both open complexes.

Factors Affecting DNase I and HO ·Reactivity (Footprinting) at a Site. The amount of reaction at a site in a fixed-time footprinting assay is determined by (i) the intrinsic rate constant for reaction with a fully accessible site, (ii) the fractional accessibility of a site, and (iii) the local concentration of the reagent at the site. In general, reactivity is reduced relative to free DNA; this reduction is termed "protection". At a limited number of sites, reactivity is increased relative to free DNA; these increases are termed "enhancements". Important considerations involved in a structural interpretation of the HO· and DNase I footprints are described below.

Intrinsic Reactivity. DNase I binds in the minor groove, contacting a total of six phosphates (two from one strand, four from the other) over six base pairs (bp) (Suck et al., 1988). DNase I cleaves the phosphodiester bond of a site at sequence-specific rates, leaving 5′-phosphate and 3′-

† This work was supported by a grant from the NIH (GM23467). M.L.C. was supported in part by an NIH Biotechnology training grant (5T32 GM08349).

* Correspondence should be addressed to this author at the Department of Biochemistry, University of Wisconsin, 420 Henry Mall, Madison, WI 53706. Phone: (608) 262-5332. Fax: (608) 262-3453. E-mail: Record@chem.wisc.edu.

‡ Department of Biochemistry.

§ Department of Chemistry.

|| Presently at the University of California-San Francisco, Department of Microbiology and Stomatology, Box 0512, San Francisco, CA 94143.

⊗ Abstract published in *Advance ACS Abstracts,* November 15, 1995.

0006-2960/95/0434-15624$09.00/0

hydroxyl ends (Stryer, 1988). Hydroxyl radicals are produced by the Fenton reaction between $Fe(EDTA)^{2-}$ and H_2O_2 (Price & Tullius, 1992). Hydroxyl radicals scavenge a hydrogen atom from the sugar ring; subsequent elimination of the DNA nucleoside leaves 5′- and 3′-phosphate ends (Price & Tullius, 1992). HO• cuts all positions of unbent B DNA with little sequence specificity.

Accessibility (Steric Effects). DNase I, which is ~40 Å in diameter (Leblanc & Moss, 1994), provides a lower resolution footprint than HO• because of steric effects. DNase I, but not HO•, may be sterically excluded from water-accessible positions. If $Fe(EDTA)^{2-}$ and/or H_2O_2 are excluded from a site, then the extent of reaction is expected to be limited by the short lifetime of HO•. Decreased cutting by both HO• (Price & Tullius, 1992) and DNase I (Drew & Travers, 1984) has been observed at A_n tracts where the width of the minor groove is thought to be reduced [reviewed in Travers (1989)].

Local Concentration of Reagent (Charge Effects). $E\sigma^{70}$ binding may locally neutralize or reinforce the high negative charge density of the DNA backbone, affecting local reactivity of both HO• and DNase I. The active site of DNase I is positively charged; three arginine side chains interact directly with an octanucleotide in a crystallized complex (Suck et al., 1988). $Fe(EDTA)^{2-}$ and ascorbate are negatively charged. A local reduction in negative charge density near the DNA backbone should increase the local concentrations of $Fe(EDTA)^{2-}$ and ascorbate, and hence of hydroxyl radicals (Lu et al., 1990; Zhong & Kallenbach, 1994), while decreasing the local concentration of the DNase I active site.

Interpretation of Enhancements. In co-crystals of DNase I with an octanucleotide (Suck et al., 1988), DNase I binding in the minor groove increases the minor groove width by 3 Å, inducing a 21.5° bend toward the major groove. This result is consistent with the observation [reviewed in Travers (1989)] that DNase I preferentially cleaves sites located in bent DNA with a widened minor groove. For example, the crystal structure of a CAP-DNA complex reveals that two DNase I hypersensitive sites are located in the widened minor groove at ~40° kinks (Schultz et al., 1991). DNase I enhancements are therefore interpreted as sites of local bending toward the major groove. Enhancements of HO• cleavage in RNA polymerase−promoter complexes have not previously been discussed. We propose that they result from greater steric accessibility and/or local reductions in negative charge density of the DNA backbone at the outwardly directed surface of a protein-induced bend.

MATERIALS AND METHODS

Enzymes and Chemicals. E. coli K12 RNA polymerase holoenzyme ($E\sigma^{70}$) was purified in this laboratory by existing methods [Burgess and Jendrisak (1975), as modified by Gonzales et al. (1977)] and stored in $E\sigma^{70}$ storage buffer [50% glycerol, 10 mM Tris (pH 7.5 at 4 °C), 100 mM $NaCl_2$, 0.1 mM dithiothreitol (DTT), 0.1 mM EDTA] at −70 °C. This preparation was determined by filter binding to be approximately 25% active; concentrations cited below refer to active holoenzyme. Magnesium chloride hexahydrate (purity 99.995%) was from Aldrich (Milwaukee, WI). Other chemicals were analytical grade.

Buffers. Binding buffer (BB) contains 10 mM potassium HEPES (pH 7.5), 50 mM NaCl, 0.1 mM EDTA, 1 mM DTT, 100 μg/mL bovine serum albumin and, when indicated, 10 mM $MgCl_2$. The concentration of the $MgCl_2$ stock was verified by inductively coupled plasma emission spectroscopy (Leeman Lab, Inc. plasma spectrometer, UW Chemistry Department). TBE contains 89 mM Tris base, 89 mM boric acid, and 2 mM EDTA. Alkaline formamide loading buffer contains 85% formamide, 10 mM NaOH, 1 mM EDTA, 0.1% xylene cyanol (XC), and 0.1% bromophenol blue (BPB). Urea loading buffer consists of 8 M urea, 0.5× TBE, 0.05% XC, and 0.05% BPB.

λP_R Promoter DNA. The λP_R promoter (−60 to +20) is contained on plasmid pBR81. A previous description of pBR81 (Suh et al., 1993) is incorrect. An 80 bp synthetic λP_R cassette was inserted into the *Hpa*I and *Sal*I sites of pBend 5 (Zwieb & Adhya, 1994) with transcription directed toward the *Sal*I site. The *Eco*RV−*Sal*I fragment from the resulting plasmid (pBR80) was ligated into the corresponding sites on pBluescript II SK(−) (Stratagene, LaJolla, CA) to make pBR81.

pBR81 was purified using a maxi kit by QIAGEN, Inc. (Chatsworth, CA) and digested with *Bss*HII, which cleaves at positions +77 and −226 relative to +1. The *Bss*HII fragment was labeled at the 3′ end of the **n** strand with [α-^{32}P]dCTP using Sequenase DNA polymerase (USB, Cleveland, OH) and alternatively at the 5′ end of the **t** strand with [γ-^{32}P]ATP using T4 polynucleotide kinase after dephosphorylation with CIP. Uniquely end-labeled, 187 bp fragments were generated by digestion with *Sma*I, which cuts at position −110 of λP_R. The λP_R containing fragments were separated from unwanted fragments by 5% polyacrylamide gel electrophoresis, band excision, and elution. They were purified and concentrated using Elutip-d columns (Schleicher and Schuell, Keene, NH).

Formation of Open Complexes. λP_R-containing DNA fragments (187 bp) were incubated at 25 °C for 20 min with a 10−60-fold excess of $E\sigma^{70}$ in 20−40 μL of BB with or without 10 mM $MgCl_2$. Based on ethidium bromide dot quantitation (Selden & Chory, 1987) of representative labelings, the DNA concentration in these experiments was approximately 0.5 nM.

Backbone Cleavage with HO•. $Fe(EDTA)^{2-}$ was prepared <2 min before starting the reactions by mixing equal volumes of 120 mM ammonium iron (II) sulfate and 240 mM Na_2EDTA (pH 8) solutions. Exactly 15 s after addition of heparin (final concentration 5 μg/mL) to the $E\sigma^{70}$−promoter complexes, reagents for HO• footprinting were added over a 15 s period in the following order: sodium ascorbate to 1 mM, H_2O_2 to 0.03%, and $Fe(EDTA)^{2-}$ [final concentrations 9 and 18 mM for Fe (II) and Na_2 EDTA, respectively]. After a 2 min incubation at 25 °C, HO• were quenched by the addition a thiourea/EDTA solution (final concentrations 9.5 mM thiourea and 1.7 mM EDTA). The DNA was ethanol-precipitated in the presence of 10 μg of glycogen, washed once with 200 μL of ice-cold 90% ethanol, and resuspended in 5−15 μL of alkaline formamide or urea loading buffer.

Three experiments were performed in the "single-hit" regime (<1 scission per DNA molecule). Control experiments were performed in which $E\sigma^{70}$ storage buffer was substituted for $E\sigma^{70}$. Because glycerol quenches HO•, the final glycerol concentration must be <3%. Therefore, the maximum $E\sigma^{70}$ concentration is limited by the 50% glycerol in the storage buffer.

Backbone Cleavage with DNase I. DNase I requires Mg^{2+} cofactor to hydrolyze the phosphodiester bonds of DNA; Ca^{2+} exhibits a marked synergistic effect with Mg^{2+} (Melgar & Goldthwait, 1968). To obtain the footprint of RP_{o1} ($-Mg^{2+}$), complexes formed in the absence of Mg^{2+} were probed with DNase I at 0.5 mM $MgCl_2$, 0.5 mM $CaCl_2$, 60−150 ng/mL DNase I for 10 s at 25 °C. $KMnO_4$ footprinting [performed as in Suh et al. (1993)] showed that these concentrations of Mg^{2+} and Ca^{2+} did not cause significant conversion of RP_{o1} to RP_{o2} under the conditions of our assay. For probing RP_{o2}, a DNase I stock containing Ca^{2+} was added to complexes formed in the presence of 10 mM Mg^{2+} (final concentrations 0.5 mM $CaCl_2$ and 40−100 ng/mL DNase I) and incubated at 25 °C for 10 s. DNase I digestions were stopped by the addition of EDTA and sodium acetate to final concentrations of 35 and 320 mM, respectively. Phenol (100 μL) was added immediately, and samples were vortexed and placed on ice until all reactions were finished. The aqueous phase was diluted to 100 μL with 0.3 M sodium acetate and prepared for gel loading as for the HO• reactions.

Control experiments were performed for both the $+Mg^{2+}$ and $-Mg^{2+}$ conditions by the protocol described above except that $E\sigma^{70}$ storage buffer was substituted for $E\sigma^{70}$. Two experiments were performed in the "single-hit" regime. Figure 4 (below) was based on the two "single-hit" experiments and a third experiment exceeding the "single-hit" limit which nevertheless was consistent with the two "single-hit" experiments. Reported DNase I cleavage sites refer to the phosphodiester bond involving the 3′-hydroxyl and the 5′-phosphate of the nucleotide, respectively, for the **n** and **t** strands.

Gel Analysis of DNA Cleavage Products. Samples were heated to 90 °C for 3−10 min, and 10 000−30 000 cpm (Cerenkov) per lane were applied to an 8% or 10% denaturing polyacrylamide gel (19:1 w/w acrylamide/bis acrylamide, 7.2−8 M urea, 0.5× TBE) with dimensions 40 cm × 33 cm × 0.4 mm. Gels were electrophoresed at 2000−2500 V for 2−4 h, dried, autoradiographed with Cronex Lightning Plus intensifying screen overnight at −70 °C, and analyzed with a Molecular Dynamics, Inc. (MD, Sunnyvale, CA) phosphorimager. G+A sequencing was performed as described by Maxam and Gilbert (1980).

Phosphorimager Analysis. Semiquantitative evaluation of the protection/enhancement of cleavage of each residue was made by comparison with control lanes lacking $E\sigma^{70}$. Graphs compared here have been normalized for small differences in gel loading using the Image QuaNT program (MD, version 4.1). Normalization was based on the two-dimensional distribution of the intensities of three or more consecutive bands outside of the footprint region. Both upstream and downstream bands were considered, and the normalization was performed using bands which minimized the observed enhancements. All normalizations were checked visually by overlaying footprint and control lane traces (e.g., Figure 2 below). These overlays were created by importing the graph coordinates from Image QuaNT into Microsoft Excel and adjusting the data set by the appropriate normalization factor.

RESULTS

HO• Footprinting. HO• was used to obtain high-resolution footprints of the DNA backbone of both the **t** and **n** strands in two $E\sigma^{70}-\lambda P_R$ binary open complexes: RP_{o1}, formed in the absence of Mg^{2+}, and RP_{o2}, formed in the presence of 10 mM Mg^{2+} (Figure 1A). Figure 1 is representative of three experiments. The pattern of cleavage of the uncomplexed DNA is quantitatively similar in both the presence and absence of Mg^{2+} (data not shown). Phosphorimager analyses demonstrate two major differences between the footprints of the DNA backbone in RP_{o1} and RP_{o2}: (i) At the start site (−4 to +1) of the **t** strand, the extent of protection of the backbone from reaction with HO• is significantly reduced in RP_{o2} relative to RP_{o1}, although these positions in RP_{o2} remain less reactive than in uncomplexed DNA. Phosphorimager analysis of the gel shown in Figure 1A is displayed in Figure 1B. (ii) On the **t** strand in RP_{o1}, reproducible enhancements of backbone cleavage relative to free DNA are observed at positions −35 to −38 and −47 to −49; the extent of enhancement is similar in the two regions. On the same strand in RP_{o2}, the extent of enhancement is much greater than in RP_{o1} at position −38, whereas the enhancements decrease significantly at positions −47 to −49 (Figure 2). No reproducible enhancements were observed on the **n** strand.

In addition to the above-mentioned specific features of RP_{o1} or RP_{o2}, other features of the HO• footprints are common to both complexes (Figure 4). For RP_{o2}, many of these features are directly comparable to those previously noted for other promoters; no previous comparison of the HO• footprints of RP_{o1} and RP_{o2} has been published. The HO• footprints of both complexes extend from at least −70 to +24. Both the open and initial transcribed regions are continuously protected from −19 to +24 on the **n** strand and from −12 to +24 on the **t** strand (with the exception of positions −4 to +1 in RP_{o2}). In the upstream region, from −13 to −70, moderately protected regions separate strongly protected regions from regions which are weakly protected, unprotected, or even enhanced. The backbones of approximately 6−7 out of every 11 nucleotides are strongly or moderately protected from HO• cleavage. This periodic pattern of protection spans five helical turns with a periodicity similar to that of the DNA helix (~11 bp). Positions of relative maxima (and also of relative minima) in the protection pattern are offset by about 3 bp between the **t** and **n** strands.

DNase I Footprinting. No significant differences were observed between the DNase I footprints of RP_{o1} and RP_{o2} in three independent experiments (cf. Figure 3). Features of the DNase I footprints are also summarized in Figure 4. These features are similar to those of footprints observed in Mg^{2+}-containing buffers at other promoters (see Discussion). The most striking feature of the DNase I footprints are reproducible enhancements at −38 and at −48/−49 on the **t** strand and −43, −45, and −46 on the **n** strand. The enhancement at −38 is much stronger than the others.

The DNase I footprints extend from −57 to +20 and from −52 to +25 on the **t** and **n** strands, respectively. Like the HO• footprints, the DNase I footprints show continuous protection in the downstream region and periodic protection in the upstream region. Except at the upstream end of the footprints, binding of $E\sigma^{70}$ protects more of the promoter DNA from DNase I attack than from HO•, giving a pattern of continuous protection broken occasionally, in the upstream region, by one to five partially protected, unprotected, or enhanced sites (see Figure 4 for a comparison of the DNase I and HO• footprints).

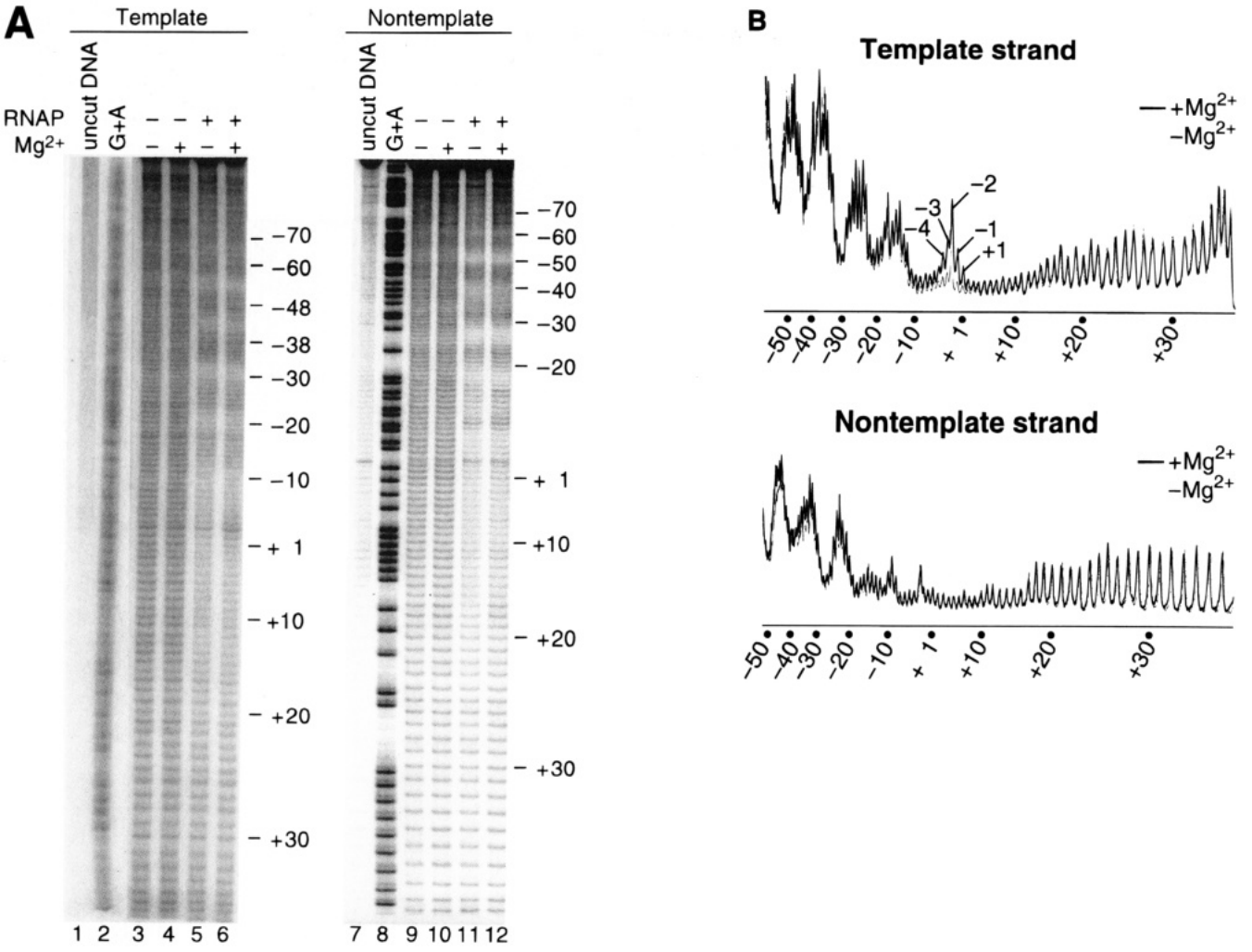

FIGURE 1: (A) Representative HO· footprints of the λP_R−Eσ^{70} complex. For both the **t** and **n** strands, representative HO· cleavage patterns of free promoter DNA in the absence (lanes 3 and 9) and presence (lanes 4 and 10) of Mg^{2+} and of the open complexes RP_{o1} ($-Mg^{2+}$) (lanes 5 and 11) and RP_{o2} ($+Mg^{2+}$) (lanes 6 and 12) at 25 °C are shown. (G + A)-sequencing (Maxam & Gilbert, 1980; lanes 2 and 8) and uncut DNA controls (lanes 1 and 7) were performed for both strands. (B) Increased accessibility of the transcription start site in RP_{o2} vs RP_{o1}. The HO· footprints in Figure 1A were quantified using a Molecular Dynamics phosphorimager. The scans of RP_{o1} and RP_{o2} were compared for both the **t** (lanes 5 and 6) and **n** (lanes 11 and 12) strands.

DISCUSSION

Unique Features of RP_{o1} and the Conversion to RP_{o2}. Conversion of RP_{o1} to RP_{o2} at λP_R requires the uptake of ~3 Mg^{2+} ions (Suh et al., 1992). We have exploited this requirement in order to footprint these two open complexes individually and to compare their structural properties. In this section, we consider our novel HO· and DNase I footprinting data in the context of previous $KMnO_4$ data (Suh et al., 1993) on RP_{o1} and RP_{o2} at λP_R and structural data on Eσ^{70} and other polymerases (referenced below) to develop a model for the events accompanying Mg^{2+} binding to form the final binary open complex (RP_{o2}) on the path to transcription initiation.

In RP_{o1}, the sugar−phosphate backbones of both DNA strands in the vicinity of the start site are strongly (moderately at −2) protected from both HO· and DNase I (Figures 1A and 3). However, many of the pyrimidine bases on both strands in this region are at least somewhat reactive to MnO_4^-, which reacts with unpaired or distorted pyrimidines (Hayatsu & Ukita, 1967; Borowiec et al., 1987). In particular the −4, −3, and (to a lesser extent) +2 thymines on the **n** strand and the −8, −9, and −11 thymines and the −12 cytosine on the **t** strand exhibit some reactivity with MnO_4^- in the absence of Mg^{2+}. Suh et al. (1993) concluded that the reactive bases in the region immediately upstream of the start site (from at least −3 to −12) were unpaired and were incompletely protected from MnO_4^- by interactions with Eσ^{70}. Thymines, at −7 and −10 on the **n** strand are unreactive, suggesting that they may be unpaired but protected by Eσ^{70}.

Upon uptake of ~3 Mg^{2+} ions (Suh et al., 1992), the −4 to +1 backbone and the +1 thymine on the **t** strand become accessible to HO· (Figure 1) and MnO_4^-, respectively, and the MnO_4^- reactivity of already reactive pyrimidines increases. Because in RP_{o1} the +1 thymine is unreactive and the +2 thymine is only weakly reactive, and because the increase in MnO_4^- reactivity in the conversion to RP_{o2} is large at these positions, Suh et al. (1993) concluded that the bases at the start site (+1, +2) became unpaired in a conformational change accompanying Mg^{2+} binding. Alternatively, if the weak reactivity of the +2 thymine in RP_{o1} signifies that this position is unpaired but partially protected by Eσ^{70}, then the entire region (+2 to −12) may be unpaired in RP_{o1}. In this case, the increased reactivity to MnO_4^- at positions +1 and +2 in RP_{o2} may result from increased steric access of the reagent and/or an increase in the local

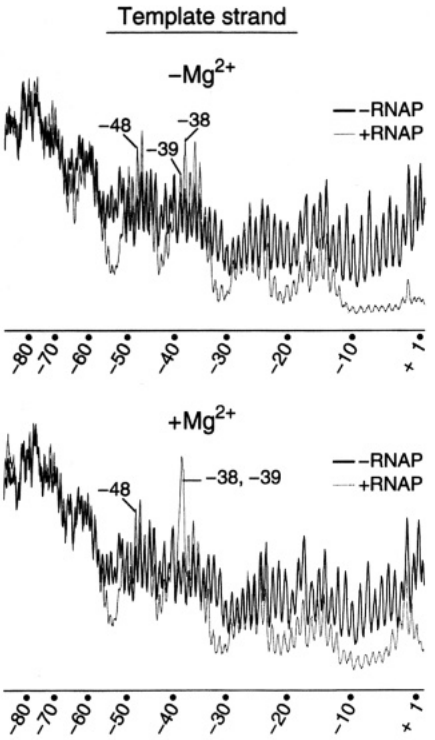

FIGURE 2: Differences in enhancements of HO· cleavage in RP_{o1} and RP_{o2}. Each footprint lane was compared with its respective control lane lacking $E\sigma^{70}$. For the **t** strand, the RP_{o1} and RP_{o2} footprints (light lines) are compared with their respective uncomplexed DNA control (heavy lines) lacking or containing Mg^{2+}.

concentration of the reagent accompanying the binding of Mg^{2+}.

The existence of two crucially important Mg^{2+} binding sites near the start site can be inferred by analogy to structural studies on other polymerases. In the *E. coli* DNA polymerase Klenow fragment, rat DNA polymerase β, HIV reverse transcriptase, and T7 and T7/T3 RNA polymerases, a cleft between finger- and thumb-like structures (described as the palm of a hand) contains two aspartates and, in some cases, a third carboxylate residue, which serve as sites for complexing two Mg^{2+} ions (Pelletier et al., 1994; Steitz et al., 1994). Two homologous aspartates are invariant among three families of DNA-dependent DNA polymerases (pol I, pol α, and pol β), RNA-dependent DNA and RNA polymerases, and the single-subunit RNA polymerases (Delarue et al., 1990). Candidates for analogous sites on $E\sigma^{70}$ have been identified by cross-linking studies and mutational analysis; aspartates 460, 462, and 464 on β' and glutamates 1272 and 1274 on β appear to be involved in nucleotide binding and may serve as sites of Mg^{2+} complexation (A. Goldfarb and A. Mustaev, personal communication).

Sousa et al. (1993) propose that a catalytic pocket on T7 RNA polymerase contains the two invariant aspartates and that this pocket is located near the +1 site during transcription initiation. A similar pocket on $E\sigma^{70}$ may surround the −4 to +1 nucleotides on the **t** strand. In addition to the carboxylate residues implicated in nucleotide (and possibly Mg^{2+}) binding, histidine 1237 and lysine 1065 (Mustaev et al., 1991) and lysine 1234 or 1242 (Grachev et al., 1989) of β and region 3 of σ^{70} (Severinov et al., 1994) are reported to be part of the catalytic center and may also lie in the catalytic pocket. In a model where the conversion from RP_{o1} to RP_{o2} results from charge effects alone, local negative

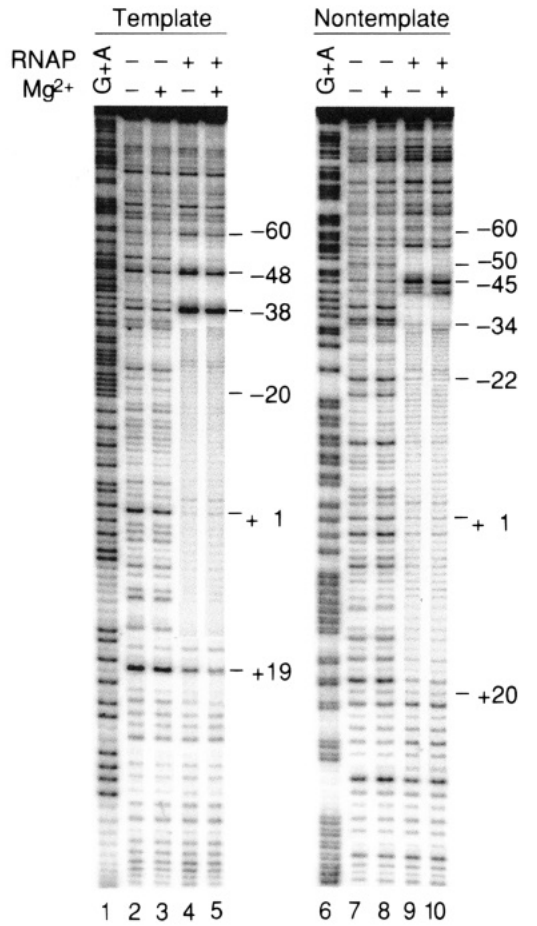

FIGURE 3: Representative DNase I footprints of the λP_R−$E\sigma^{70}$ Complex . For both the **t** and **n** strands, representative DNase I cleavage patterns of free promoter DNA in minimal (0.5 mM, lanes 2 and 7) and 10 mM (lanes 3 and 8) Mg^{2+} and of the open complexes RP_{o1} (lanes 4 and 9) and RP_{o2} (lanes 5 and 10) at 25 °C are shown. (G+A)-sequencing ladders are shown in lanes 1 and 6.

charge density due to the $E\sigma^{70}$ carboxylates and DNA phosphates may be localized in this pocket in RP_{o1}, excluding $Fe(EDTA)^{2-}$ and MnO_4^-. Because they react with MnO_4^-, **n** strand thymine bases at −4 and −3 (and perhaps +2) are evidently outside of the region of high local negative charge density. The positively charged DNase I active site must be sterically excluded from cutting the +1, −2, −3, and −4 positions on the **t** strand in RP_{o1}.

If two Mg^{2+} ions bind near +1 in the conversion to RP_{o2} (as shown in Figure 5), then it is possible that increases in local concentrations of $Fe(EDTA)^{2-}$/HO· and MnO_4^- are entirely responsible for the increases in backbone and base reactivity at the start site. However, a conformational change in the $E\sigma^{70}$−λP_R complex probably accompanies Mg^{2+} binding, increasing the steric accessibility of HO· and MnO_4^- (and nucleotides) to the start site. The reduction of local negative charge density resulting from Mg^{2+} binding may also facilitate binding of the initiating nucleotide(s) by increasing the local concentration of the these oligoanions at the start site.

In addition to the changes in HO· protection at the start site, changes in the HO· protection pattern distant from the start site are observed. At positions of enhancements (∼−38, −48) corresponding to DNA bends, HO·, but not DNase I, exhibits a significant change in reactivity in the conversion to RP_{o2}. While DNase I detects similar amounts of enhancement of these positions in both complexes (Figure

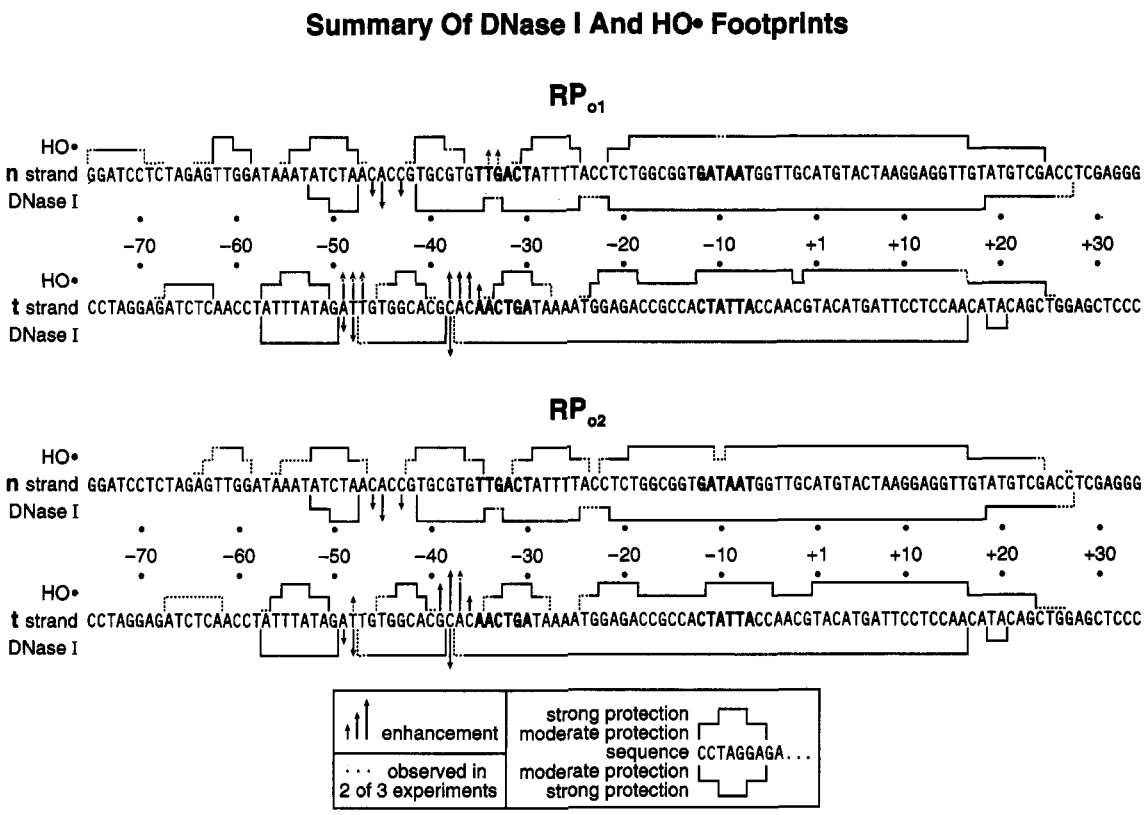

FIGURE 4: Summary of DNase I and HO• footprints of RP_{o1} and RP_{o2} at λP_R. The protection patterns of the triplicate DNase I and HO• footprinting experiments are summarized in relation to the λP_R sequence. HO• and DNase I protections are respectively illustrated above and below the sequence of each strand. Protections are divided into two categories, moderate and strong, represented by lower and upper level steps, respectively. Enhancements are shown as arrows: small, medium, and large arrows indicate weak, moderate, and strong enhancements, respectively. Dotted lines refer to positions where some inconsistency in the triplicate results was observed; the behavior observed in two of the three trials is represented. Dotted lines immediately above the sequence (no step) indicates that the position was unprotected or weakly protected in two experiments but moderately protected in the third. The −10 and −35 regions of the promoter are shown in bold.

3), the HO• enhancements from −47 to −49 in RP_{o1} decrease in the conversion from RP_{o1} to RP_{o2}, while the enhancement at −38 increases significantly (Figure 2). Since the stoichiometry of Mg^{2+} binding (uptake of ~3 Mg^{2+} ions; Suh et al., 1992) may exceed that expected at the start site (2 Mg^{2+}), it is possible that binding of an additional Mg^{2+} ion near −38 accompanies increased bending at this position, resulting in the large enhancement of HO• reactivity (Figure 5). The effects of Mg^{2+} binding and increased bending could compensate to yield no effect on DNase I reactivity; increased steric access might compensate for decreased coulombic attraction. The reduction of HO• enhancement at −47 to −49 may be caused by a conformational change in which local bending is reduced, decreasing steric accessibility to the sites. The conformational perturbation may also increase the local density of phosphates, increasing the local negative charge density and decreasing the local concentration of HO•.

Several related studies exist in other systems. Kuwabara and Sigman (1987) interpreted a Mg^{2+}-dependent increase in 1,10-phenanthroline copper reactivity at positions −3 to −6 of *lac*UV5−Eσ^{70} complexes as a transition from a closed to an open complex. Meier et al. (1995) probed T7 A1−*Thermotoga maritima* RNA polymerase complexes with OsO_4 bipyridine and saw a conversion similar to that observed by Suh et al. (1993). Straney and Crothers (1985, 1987) reported gel shift and footprinting evidence for two different *lac*UV5−Eσ^{70} open complexes in Mg^{2+}; the relationship of these complexes to those studied here is unclear.

Features Common to Both RP_{o1} and RP_{o2}. While backbone contacts in RP_{o1} have not previously been studied, backbone contacts in RP_{o2} (binary open complexes in the presence of Mg^{2+}) have been studied at many promoters. DNase I and HO• footprinting features that are similar between RP_{o1} and RP_{o2} at λP_R (Figure 4) are also common features of RP_{o2} complexes at other promoters. The principal conserved features have been incorporated into Figure 5 and are as follows: (1) continuous protection including and downstream of the −10 region, (2) periodic variation in the degree of protection upstream of the −10 region, (3) the approximate position of the division between the regions of periodic and full protection, (4) enhancements of cleavage at several promoter-specific positions, and (5) the approximate upstream and downstream footprint boundaries. We expect that RP_{o1} complexes at other promoters will exhibit these characteristics. The implications of conserved features 1−5 on the structure of the Eσ^{70}−promoter complexes are discussed below.

The promoters included in the following discussion are as follows: DNase I footprinting, lac UV5 (Kovacic, 1987; Carpousis & Gralla, 1985; Kolb et al., 1993; Spassky et al., 1985), rrnB P1 (Newlands et al., 1991; Ross et al., 1993), f_d PVIII (Hofer et al., 1985), T7 A3 (Kovacic, 1987), groE, rpoD P_{HS}, and dnaK P2 (Cowing & Gross, 1989); hydroxyl radical footprinting, groE, rpoD P_{HS}, and dnaK P2 (Mecsas

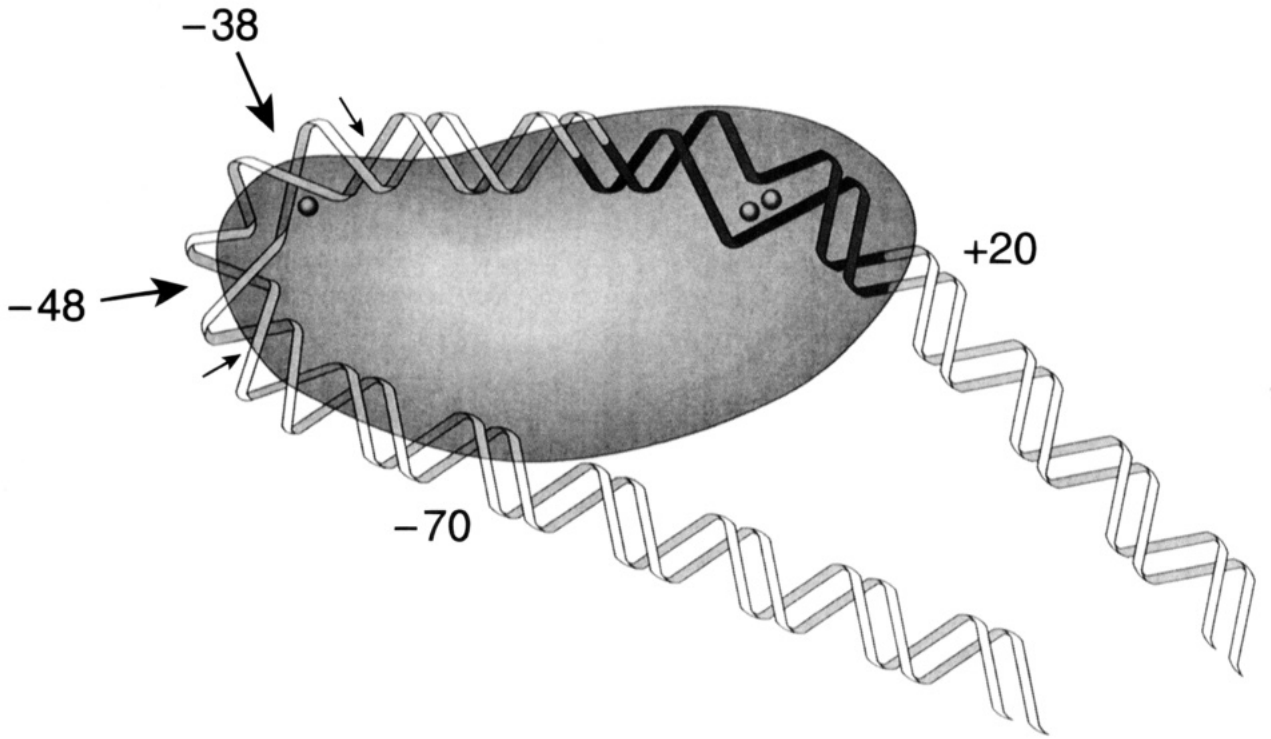

FIGURE 5: 2D Model for the $\lambda P_R-E\sigma^{70}$ open complex (RP_{o2}). The model was drawn approximately to scale: 18 Å = 1 cm. λP_R promoter DNA was positioned on a cartoon protein of the approximate dimensions (160 Å × 100 Å) determined by Darst et al. (1989). In the upstream region, four DNA bends result in the wrapping of DNA around the protein. The small arrows show intrinsic DNA bends at A_n/T_n tracts; the large arrows show protein-induced bends. Spheres (not drawn to scale) indicate possible binding sites for the three Mg^{2+} ions (Suh et al., 1992) taken up in the conversion from RP_{o1} to RP_{o2}. An approximately 45° bend is included at +1 based on the study of Meyer-Almes et al. (1994).

et al., 1991), rrnB P1 (Newlands et al., 1991), merR and merT (O'Halloran et al., 1989), lac UV5 (Kolb et al., 1993), and T7 A1 (Schickor et al., 1990).

(1) Backbone protection in the downstream region is continuous except at the start site. Most of the DNA backbone on both strands is strongly protected from cleavage by both HO· and DNase I in the downstream region (∼−10 to +25, or a total of ∼70 nucleotides). For λP_R and the promoters cited above, DNase I footprints show complete or partial protection on both strands at virtually every position in this region; HO· footprinting shows complete protection at every position on the **n** and **t** strands except promoter-specific sites on the **t** strand in the vicinity of the start site. The details of HO· accessibility of the **t** strand backbone near the start site appear to be promoter-specific. At λP_R, the **t** strand is partially accessible from −4 to +1 in RP_{o2} but not RP_{o1}. Similarly, the **t** strand at P_{merR} and P_{merT} [$E\sigma^{70}$ binds at P_{merT} only in the presence of the activator MerR and Hg(II)] is slightly accessible to HO· from −3 to −1 and from −3 to +1, respectively, in the presence of 2 mM Mg^{2+} (O'Halloran et al., 1989). [Unpublished experiments on λP_R (W.-C. Suh and M. T. Record, Jr.) indicate that incomplete conversion of RP_{o1} to RP_{o2} occurs at this Mg^{2+} concentration.] The T7 A1 promoter shows significant HO· reactivity from −7 to +2 on the **t** strand in an open complex in the absence of Mg^{2+} (Schickor et al., 1990). For complexes of $E\sigma^{32}$ with various heat shock promoters [groE, rpoD P_{HS}, and dnaK P_2 (Mecsas et al., 1991); rpoD P_{HS} showed anomalous reactivity at −2] and for $E\sigma^{70}$ at rrnB P1 (in the presence of ATP, CTP; Newlands et al., 1991), complete protection of the start site on both strands is observed in the presence of 10 mM Mg^{2+}.

(2) Backbone protection is periodic in the upstream region. The periodicity of HO· protection observed in the upstream region of λP_R is a general feature of HO· footprints of σ^{70} (and σ^{32}) promoters (references cited above). The period of this repeat is, on average, 11 ± 2 bp, similar to the 10.5 bp helical repeat of B DNA. This period indicates that $E\sigma^{70}$ is binding to one side of the DNA helix (Tullius et al., 1987). An ∼3 bp offset in the footprint patterns between the **n** and **t** strands indicates residues which are located across the minor groove from one another (Tullius & Dombroski, 1986).

An important feature of the HO· protection pattern that has not previously been discussed is the large number of positions per helical turn that are protected. For λP_R, 6−7 out of each 11 bp are either strongly or moderately protected from HO· cleavage. Qualitative examination of published HO· footprints (cited above) indicate that, on average, at least 5 out of every 11 bp are strongly or moderately protected. One possible interpretation of this result is that periodically spaced protrusions from the protein surface, such as the helix−turn−helix motif of σ^{70} believed to interact with the −35 region (Siegele et al., 1989; Gardella et al., 1989), interact with one side of the DNA helix. Such protrusions from the surfaces of Cro protein (Mondragon & Harrison, 1991) and λ repressor (Beamer & Pabo, 1992) cause a periodic HO· protection pattern similar to, but shorter than, that observed in the upstream region of λP_R (Tullius & Dombroski, 1986). A second interpretation, which we favor, is that the DNA lies in an extensive groove on the surface of the polymerase molecule. The crystal structure (at 3.1 Å resolution) of the nucleosomal core histone octamer shows grooves which are thought to bind the nucleosomal DNA

(Arents et al., 1991); the DNase I and HO· protection patterns of nucleosomal DNA (Hayes et al., 1990) display periodicity similar to that of the upstream region of λP_R when complexed with $E\sigma^{70}$. Since $E\sigma^{70}$ protects at least half of the backbone of each helical turn, the groove on $E\sigma^{70}$ must be at least as wide as the diameter of the DNA helix (~20−25 Å) and at least as deep as the radius (10−12 Å). In order for the groove to periodically protect five helical turns, its length must be about 170 Å. Darst et al. (1991) deduced the existence of a more limited groove of this width and depth from low-resolution electron microscopy on the homologous (Allison et al., 1985; Sweetser et al., 1987) yeast RNA polymerase II [reviewed in Record et al. (1996)]. The three-dimensional electron crystallography structures of both $E\sigma^{70}$ (Darst et al., 1989) and *E. coli* core RNA polymerase (Polyakov et al., 1995) show multiple grooves on the surface of both molecules. One or more of the observed grooves is presumably responsible for binding the upstream promoter region.

(3) Division between regions of periodic and full protection of the backbone. The transition between periodic and continuous protection occurs between −10 and −23 for the promoters cited above. Different promoters and different probes exhibit characteristically different transition points between these two regions. For λP_R, the transition occurs at position −12 by the HO· technique and at −22 by DNase I. DNase I may be excluded from cutting the −12 to −22 region for steric reasons.

(4) Enhancements of backbone cleavage in RP_{o2}. Sites of DNase I enhancements are commonly observed in $E\sigma^{70}$ (and $E\sigma^{32}$) promoter complexes. DNase I enhancements were observed for all promoters cited above; however, the positions of these enhancements varied significantly. For λP_R, we observe enhancements at −38 and −48/−49 on the **t** strand and at −43, −45, and −46 on the **n** strand. Enhancements of HO· cleavage in any RNA polymerase promoter complex have not previously been discussed. In RP_{o2} of λP_R, we observe large, reproducible enhancements only at positions −36 to −39.

The sites of enhancement may indicate DNA positions on the "outside" of protein-induced bends. Darst et al. (1989) determined the approximate dimensions of $E\sigma^{70}$ to be 90 × 95 × 160 Å, too small to accommodate, without DNA bending, the ~340 Å (100 bp) of DNA protected from HO· cleavage. A_n tracts are putative sites of DNA bending toward the minor groove (Price & Tullius, 1992; Travers, 1989). We propose that a T_4 tract at −25 to −29 (surrounded by 3A's/T's) and an A_3 tract at −54 to −56 (surrounded by 4 A's/T's), sites of reduced cleavage relative to surrounding positions in free DNA, are bent both in free DNA and in the RNA polymerase−promoter complex. Together, the bends at the sites of enhancement and at the $A_n(T_n)$ tracts may serve to wrap the DNA around $E\sigma^{70}$ (Figure 5). Bending of the promoter DNA by $E\sigma^{70}$ has been observed by a variety of techniques: the gel electrophoretic mobility shift method (Heumann et al., 1986, 1988a; Kuhnke et al., 1987, 1989), neutron small angle scattering (Heumann et al., 1988b), scanning force microscopy (Rees et al., 1993), and quantitative electrooptics (Meyer-Almes et al., 1994). Rees et al. (1993) and Meyer-Almes et al. (1994) measured bend angles of 45° and 54° respectively, and Meyer-Almes et al. determined that the bend was centered at +1. However, neither group apparently observed the extensive bending proposed in this study. It is possible that the bend angle observed by Rees et al. is actually 360° + 54° = 394°, resulting from DNA wrapping similar to that which we propose.

(5) Upstream and downstream boundaries of the footprints. The downstream boundaries of the HO· and DNase I footprints of λP_R (+24 and +25, respectively) are similar to the ~+20 boundaries observed for the promoters cited above (except T7 A1, whose HO· boundary is +33). The upstream boundaries, −57 by DNase I and ~−65 by HO·, are within the −45 to −65 range of upstream boundaries observed by both HO· and DNase I footprinting for the promoters cited above (except −73 for lacUV5 by HO·; Kolb et al., 1993). HO· protection beyond the region of the DNase I footprint is unexpected, but not unprecedented. Other examples of DNA binding proteins whose HO· footprints extend beyond their DNase I footprints are the nucleosome (Hayes et al., 1990) and the *Xenopus* transcription factor TFIIIA (Vrana et al., 1988). The extended HO· footprint may result from one or both of the following scenarios: (i) Local protein positive charge density on the upstream end of the DNA-binding site on $E\sigma^{70}$ could decrease DNase I reactivity while increasing HO· reactivity; (ii) binding of DNase I may competitively displace weak $E\sigma^{70}$−DNA contacts in this region.

CONCLUSIONS

Because the negative charge and small size of $Fe(EDTA)^{2-}$ (i.e., HO·) are comparable to the charge and size of the RNA nucleotide substrates, we have used HO· as a probe of nucleotide access to the DNA of λP_R−$E\sigma^{70}$ complexes. HO· probing indicates that access of the initiating nucleotide(s) to the DNA start site increases in the conversion from RP_{o1} to RP_{o2}. We propose that the binding of two Mg^{2+} ions near the start site plays a key role in making the start site accessible to the initiating nucleotide(s), either by inducing a conformational change in the $E\sigma^{70}$−λP_R complex and/or by reducing local negative charge density. In the upstream promoter region, we speculate that binding of a third Mg^{2+} ion near the −38 position may locally reduce negative charge density and induce a change in two protein-induced DNA bends (at ~−38 and −48). These protein-induced bends, in combination with two intrinsic bends, appear to wrap the λP_R promoter DNA around $E\sigma^{70}$ in both RP_{o1} and RP_{o2}.

ACKNOWLEDGMENT

We acknowledge with thanks the advice of Dr. W. Ross on the footprinting techniques, the preparation of $E\sigma^{70}$ by Mike Capp with assistance from Dr. P. Schlax and K. McQuade, and discussions and comments provided by Drs. Ross, R. Gourse, P. Schlax, and R. Spolar, and K. McQuade. We also thank Drs. T. Tullius, E. P. Geiduschek, J. Helmann, H. Heumann, T. Meier, A. Mustaev, and the reviewers for their suggestions and comments on the manuscript, Drs. A. Goldfarb and A. Mustaev for permitting us to cite their work prior to publication, M. Li and Dr. H. Guttman for verifying the concentration of the $MgCl_2$ stock, and S. Aiello for preparation of the manuscript.

REFERENCES

Allison, L. A., Moyle, M., Shales, M., & Ingles, C. J. (1985) *Cell 42*, 559−610.

Arents, G., Burlingame, R. W., Wang, B.-C., Love, W. E., & Moudrianakis, E. N. (1991) *Proc. Natl. Acad. Sci. U.S.A. 88*, 10148−10152.
Beamer, L. J., & Pabo, C. O. (1992) *J. Mol. Biol. 227*, 177−196.
Borowiec, J. A., Zhang, L., Sasse-Dwight, S., & Gralla, J. D. (1987) *J. Mol. Biol. 196*, 101−111.
Burgess, R. R., & Jendrisak, J. J. (1975) *Biochemistry 14*, 4634−4638.
Carpousis, A. J., & Gralla, J. D. (1985) *J. Mol. Biol. 183*, 165−177.
Cowing, D. W., & Gross, C. A. (1989) *J. Mol. Biol. 210*, 513−520.
Darst, S. A., Kubalek, E. W., & Kornberg, R. D. (1989) *Nature 340*, 730−732.
Darst, S. A., Edwards, A. M., Kubalek, E. W., & Kornberg, R. D. (1991) *Cell 66*, 121−128.
Delarue, M., Poch, O., Tordo, N., Moras, D., & Argos, P. (1990) *Protein Eng. 3*, 461−467.
Drew, H. R., & Travers, A. A. (1984) *Cell 37*, 491−502.
Gardella, T., Moyle, H., & Susskind, M. M. (1989) *J. Mol. Biol. 206*, 579−590.
Gonzales, N., Wiggs, J., & Chamberlin, M. J. (1977) *Arch. Biochem. Biophys. 182*, 404−408.
Grachev, M. A., Lukhtanov, E. A., Mustaev, A. A., Zaychikov, E. F., Abdukayumov, M. N., Rabinov, I. V., Richter, V. I., Skoblov, Y. S., & Chistyakov, P. G. (1989) *Eur. J. Biochem. 180*, 577−585.
Hayatsu, H., & Ukita, T. (1967) *Biochem. Biophys. Res. Commun. 29*, 556−561.
Hayes, J. J., Tullius, T. D., & Wolffe, A. P. (1990) *Proc. Natl. Acad. Sci. U.S.A. 87*, 7405−7409.
Hofer, B., Muller, D., & Koster, H. (1985) *Nucleic Acids Res. 13*, 5995−6013.
Kolb, A., Igarashi, K., Ishihama, A., Lavigne, M., Buckle, M., & Buc, H. (1993) *Nucleic Acids. Res. 21*, 319−326.
Heumann, H., Metzger, W., & Niehorster, M. (1986) *Eur. J. Biochem. 158*, 575−579.
Heumann, H., Ricchetti, M., & Werel, W. (1988a) *EMBO J. 7*, 4379−4381.
Heumann, H., Lederer, H., Baer, G., May, R. P., Kjems, J. K., & Crespi, H. L. (1988b) *J. Mol. Biol. 201*, 115−125.
Kovacic, R. T. (1987) *J. Biol. Chem. 262*, 13654−13661.
Kuhnke, G., Fritz, H. J., & Ehring, R. (1987) *EMBO J. 6*, 507−513.
Kuhnke, G., Theres, C., Fritz, H. J., & Ehring, R. (1989) *EMBO J. 8*, 1247−1255.
Kuwabara, M. D., & Sigman, D. S. (1987) *Biochemistry 26*, 7234−7238.
Leblanc, B., & Moss, T. (1994) in *DNA−Protein Interactions, Principles and Protocols* (Kneale, G. G., Eds.) pp 1−10, Humana Press, Totowa, NJ.
Lu., M., Guo, Q., Wink, D. J., & Kallenbach, N. R. (1990) *Nucleic Acids Res. 18*, 3333−3337.
Maxam, A. M., & Gilbert, W. (1980) *Methods Enzymol. 65*, 499−560.
Mecsas, J., Cowing, D. W., & Gross, C. A. (1991) *J. Mol. Biol. 220*, 585−597.
Meier, T., Schickor, P., Wedel, A., Cellai, L., & Heumann, H. (1995) *Nucleic Acids Res. 23*, 988−994.
Melgar, E., & Goldthwait, D. A. (1968) *J. Biol. Chem. 243*, 4409−4416.
Meyer-Almes, F. J., Heumann, H., & Porschke, D. (1994) *J. Mol. Biol. 236*, 1−6.
Mondragon, A., & Harrison, S. C. (1991) *J. Mol. Biol. 219*, 321−334.
Mustaev, A., Kashlev, M., Lee, J., Polyakov, A., Lebedev, A., Zalenskaya, K., Grachev, M., Goldfarb, A., & Nikiforov, V. (1991) *J. Biol. Chem. 266*, 23927−23931.
Newlands, J. T., Ross, W., Gosink, K. K., & Gourse, R. L. (1991) *J. Mol. Biol. 220*, 569−583.
O'Halloran, T. V., Frantz, B., Shin, M. K., Ralston, D. M., & Wright, J. G. (1989) *Cell 56*, 119−129.
Pelletier, H., Sawaya, M. R., Kumar, A., Wilson, S. H., & Kraut, J. (1994) *Science 264*, 1891−1903.
Polyakov, A., Severinova, E., & Darst, S. A. (1995) *Cell* (in press).
Price, M. A., & Tullius, T. D. (1992) *Methods Enzymol. 212*, 194−219.
Record, M. T., Jr., Reznikoff, W. S., & Schlax, P. J. (1996) in *Escherichia coli and Salmonella typhimurium: Cellular and Molecular Biology*, second ed., American Society for Microbiology, Washington, D.C.
Rees, W. A., Keller, R. W., Vesenka, J. P., Yang, G., & Bustamante, C. (1993) *Science 260*, 1646−1649.
Ross, W., Gosink, K. K., Salomon, J., Igarashi, K., Zou, C., Ishihama, A., Severinov, K., & Gourse, R. L. (1993) *Science 262*, 1407−1413.
Schickor, P., Metzger, W., Werel, W., Lederer, H., & Heumann, H. (1990) *EMBO J. 9*, 2215−2220.
Schultz, S. C., Shields, G. C., & Steitz, T. A. (1991) *Science 253*, 1001−1007.
Selden, R. F., & Chory, J. (1987) in *Current Protocols in Molecular Biology* (Ausubel, F. M., Brent, R., Kingston, R. E., Moore, D. D., Seidman, J. G., Smith, J. A., & Struhl, K., Eds.) pp 2.6.7, John Wiley & Sons, Inc., New York.
Severinov, K., Fenyo, D., Severinova, E., Mustaev, A., Chait, B. T., Goldfard, A., & Darst, S. A. (1994) *J. Biol. Chem. 269*, 20826−20828.
Siegele, D. A., Hu, J. C., Walter, W. A., & Gross, C. A. (1989) *J. Mol. Biol. 206*, 591−603.
Sousa, R., Chung, Y. J., Rose, J. P., & Wang, B.-C. (1993) *Nature 364*, 593−599.
Spassky, A., Kirkegaard, K., & Buc, H. (1985) *Biochemistry 24*, 2723−2731.
Steitz, T. A., Smerdon, S. J., Jäger, J., & Joyce, C. M. (1994) *Science 266*, 2022−2025.
Straney, D. C., & Crothers, D. M. (1985) *Cell 43*, 449−459.
Straney, D. C., & Crothers, D. M. (1987) *J. Mol. Biol. 193*, 279−292.
Stryer, L. (1988) *Biochemistry*, pp 655−656, W. H. Freeman and Co., New York.
Suck, D., Lahm, A., & Oefner, C. (1988) *Nature 332*, 464−468.
Suh, W. C., Leirmo, S., & Record, M. T., Jr. (1992) *Biochemistry 31*, 7815−7825.
Suh, W.-C., Ross, W., & Record, M. T., Jr. (1993) *Science 259*, 358−361.
Sweetser, D., Nonet, M., & Young, R. A. (1987) *Proc. Natl. Acad. Sci. U.S.A. 84*, 1192−1196.
Travers, A. A. (1989) *Annu. Rev. Biochem. 58*, 427−452.
Tullius, T. D., & Dombroski, B. A. (1986) *Proc. Natl. Acad. Sci. U.S.A. 83*, 5469−5473.
Tullius, T. D., Dombroski, B. A., Churchill, M. E. A., & Kam, L. (1987) *Methods Enzymol. 155*, 537−558.
Vrana, K. E., Churchill, M. E. A., Tullius, T. D., & Brown, D. D. (1988) *Mol. Cell. Biol. 8*, 1684−1696.
Zhong, M., & Kallenbach, N. R. (1994) *J. Biomol. Struct. Dyn. 11*, 901−911.
Zwieb, C., & Adhya, S. (1994) in *DNA−Protein Interactions, Principles and Protocols* (Kneale, G. G., Eds.) pp 281−294, Humana Press, Totowa, NJ.

BI9519765